Time Dependence of Orbital Inclination for Selected Isolated Detached Binaries

Edward H. Berkowitz
3633 Ramona Circle, Palo Alto, CA; cptphys@gmail.com

Received November 7, 2023; revised March 16, 2024; accepted April 16, 2024

Abstract Time dependence of orbital inclination is examined for twelve nominally isolated, detached eclipsing binaries having published light curves acquired over intervals of thousands of orbits or more. The stars presented here are: α CrB, V526 Sgr, QX Car, AR Cas, FT Ori, V346 Cen, AI Hya, AG Per, YZ Cas, β Aur, MY Cyg, and RZ Cha. In uniform treatment based upon a common reference set of orbital and absolute properties for each binary, uniform processing of observational histories yields apparent nutation per orbit from iterative fitting based upon precise reference parameters of a complete solution from the literature. Analytic weighting of each light curve is based upon fidelity to (WD) modeling, including corresponding absolute and orbital cited reference parameters. Empirical time dependence of orbital inclination is consistent with theoretically predicted combination of (a) long term exponentially decreasing misalignment of constituent rotations, and (b) short term periodic variation of precession associated nutation of eccentric orbits. Relative empirical nutation rate for these isolated binaries is in the range of 10^{-4}–10^{-6} °/orbit. Nearly synchronous circular orbit (nominally isolated) binaries (YZ Cas, β Aur, MY Cyg, RZ Cha) exhibit minimal but non-vanishing inclination rates.

1. Introduction

The orbital inclination of a binary, derived from independent observations acquired over an interval of thousands of orbits, is often deemed in agreement with prior determinations within observational uncertainty. In this work original observations are homogeneously processed and the relative uncertainties are analytically determined. The targets for this survey are selected detached (and nominally isolated) eclipsing binaries, well-studied over long intervals of orbital cycles and having known absolute properties, often known to parts per hundred or better. For these targets, the orbital inclination rate combines (a) slow (long time scale) monotonic approach to alignment of orbital and constituent rotation axes, and (b) precession associated nutation, i.e. periodical effects on a time scale depending upon the ratio of constituent rotational to orbital angular momentum, per Alexander (1976).

For binary stars, the two-body gravitational interaction (perturbed by tidal effects) characterizes the gravitational interaction. The selection here of isolated binaries is problematic in that the criterion is an absence of published evidence for a bound third body. Relatively isolated two-body systems, free of significant third-body perturbation, provide (in principle) limiting environments for tests of subtle gravitational effects and possibly other phenomena. It is well known that the principal perturbing phenomena is of tidal origin and for non-circular asynchronous binaries, precession-associated nutation adds to the inclination. Additional (possible) subtle phenomena are thus effectively masked. Precession and associated nutation are consequent from non-alignment of rotation axes with the orbital axis. The effect is quite small but of consequence to the subject of the present work. The effect is treated by Alexander (1976, see his Figure 6) and was noted in passing by Shakura (1985, penultimate paragraph). Tidal effects mask our ability to examine the presence or absence of anomalies characterizing the gravitational interaction. For fully circular orbit synchronous binaries, precession-associated nutation vanishes and while tidal forces continue, orbital inclination is expected to stabilize.

Section 2 describes the matter of deriving orbital inclination at different epochs from observations by various investigators in a uniform manner with attention to essential weighting of the various observations. The role of weighted linear regression (WLR) as a practical tool herein is discussed. Section 3 enumerates the several targets of the survey, together with associated tables and graphical depictions of time dependence of orbital inclination. Section 4 presents a discussion of results.

2. Method

2.1. Procedure

This orbital inclination time dependence study is based on reliable comparison of photometry of record over the period of available photometric instrumentation. In the present work that comparison is predicated on: (1) a model and a common set of absolute and orbital parameters, and (2) a quantitative measure of fidelity to that model and parameter set from which reliable relative weights are determinable. For each binary studied, a complete solution from the literature, of spectroscopic and photometric observation, is selected as the reference parameter set. With that parameter set, observations comprising each light curve (LC) of various epochs are fit via the model. For the present work the model selected is Wilson and Devinney (WD; 1971). Alternate independent iterations of relative inclination (i_c) and argument of periastron (ω) provide a corresponding sequence of values for ω and i_c. Note the subscript "c" intended to emphasize the comparative relation to the inclination parameter of the published complete solution. A differential comparison algorithm reaches an adjusted value for a first variable (ω) at the increase of rms error. The differential comparison algorithm is then separately operative upon the second variable (i_c), subject to the preceding value for ω. The standard deviation of residuals, S, for the current value of i_c is determined and the

iteration sequence continues. The cycle of alternate iterations terminates when standard deviation of residuals of i_c reach a minimum (S_{min}), indicated by a larger value of S in the next iteration of i_c. The fitted value (i_c) and the weight to be accorded (S_{min}^{-1}) are thus determined. The i_c values are proxies for actual inclination and do not supersede determinations from the literature. The rate of change in orientation per orbit, the quantitative product of this work, is determined from i_c values. Correction of published orientation, if desired, is then available as displaced in time from the reference orbit 0.

Note that the converged value of i_c is partly determined by the immediately prevailing value of ω which converges at a slightly different value. That distinction is negligible for the present purpose.

The present work assumes relatively stationary values for other (reference) parameters of each of the subject binaries during corresponding observation periods, an assumption that invites scrutiny.

An RJD parameter labeling the epoch of a subject LC is obtained as the centroid of the sequence of observation times comprising that LC. This provides a nominal position on a chronological axis denominated in orbital cycles relative to the reference LC. Each LC should be regarded as containing an uncertainty in time dependent upon the duration of that LC acquisition. An observing campaign lasting several years will exhibit a value of ω, averaged over a greater interval of apsidal motion if the entire set of observations is used. In this study some observed LC data sets have been truncated to avoid lengthy gaps in observation. For some densely populated LCs, a substantial part of one of the out-of-eclipse phase portions also may be truncated in phase. For single orbit observations at regular cadence, the median RJD labels the epoch. Where observations were published by phase only, textual clues are employed to obtain a suitable approximation for the LC epoch, or assigned from a fitted value of ω for that binary.

Note that the word "inclination" herein refers most often to the angle of the orbital plane to edge-on in the observational sense. Theoretical bases of this property will sometimes reference the angular difference of orbital and equatorial plane of a constituent body.

2.2. Weighted linear regression

For a given target, relationship over time of the several values of i_c is conveniently established with weighted linear regression (WLR). Initially this is merely a convenient model-independent metric and is a reasonable lowest order approximation for average nutational motion (with exceptions discussed below). This relationship is specifically not suggestive of a causal relationship. Absent tertiary perturbation, the predominant mechanism for evolution of orbital elements is of tidal origin, a decidedly non-linear mechanism in combination with precession-associated nutation. The evolutionary inclination rate is well-represented by a declining exponential function on a time scale of Myr. The precession period depends on angular velocity and unobservable properties of the rotating body. Precession-associated nutation occurs over sub-periods, inexpressible in closed form, but shown to be of order 10^3 orbits for several systems. This phenomenon was specifically treated by Alexander (1976) and is referenced herein as precession-associated nutation. A straight-line segment well-approximates intervals of the study period(s) superimposed on the evolutionary time scale. For precession-associated nutation, amplitudes have been shown to be of the order of several tenths of a degree. Over time scales of order 10^3 orbits, an appropriate WLR provides a reasonable averaging of inclination rate for (isolated) detached binaries. Deviations of the order of tenths of a degree from this average may be expected.

Weighting an inclination value follows residual analysis of fitting an LC through (here separate) iterations of inclination and ω. From a sequence of iterations the minimum of the standard deviation of residuals, S_{min}, is located as noted above; see Kallrath and Milone (2009). The S_{min} value is a metric for fidelity of that LC (with fitted i_c) to the model with reference parameters, and its inverse is taken as weight for the derived value of i_c. The WLR coefficient may be regarded as a concise quantitative description of the distribution of average relative orbit orientation over the interval of study. Binary orbit inclination in the context of a precessional time scale was shown to be periodic by Alexander (1976). He found amplitudes of order several tenths of a degree over (of order) ~10^3 orbit time scales, small in relation to precession periods. Hut (1981) finds exponential decrease of inclination rate over an evolutionary time scale (large in relation to precession period). Any short interval time segment, such as the present study, approximates Hut's long term decreasing exponential model in a straight line. With thousands of orbits in duration, a few tenths of a degree amplitude, and sparse data points, WLR is a reasonable approximation on the appropriate time and angular increment scale. The WLR coefficient is regarded herein as an empirical metric for composite time dependence of inclination, bearing in mind that the time dependence is a combination of a long term monotonic function and a short term periodic function (and perhaps other causation). Uncertainty in WLR coefficient, here determined, is standard error as generally obtained in least squares operations. The various WLR parameters determined herein are summarized in Table 13a.

All WLR parameterizations of eccentric orbits should be regarded as epoch-specific to the study interval due to the periodic nature of precession-associated nutation.

2.3. Process specifics

Limb-darkening coefficients are functions of effective temperature of the body and observational filter properties. Where appropriate, the same limb-darkening parameters are used where the same nominal filter was employed for the reference binary or equivalent. In other cases double interpolations of the tabulation of van Hamme (1993) served.

Specific plotted data points may be identified from apparent figure coordinates and the associated table.

2.4. Sources

Apart from conventional journal references, LCs were accessed from the AAVSO International Database (Kloppenborg *et al.* 2023, further identified with observer codes; see Table 1); the broad sky surveys ASAS3 (Pojmański *et al.* 2005) and ASAS-SN (Jayasinghe *et al.* 2019); and missions such as

Table 1. Observations from the AAVSO International Database (Kloppenborg (2023) used in this study.

Observer	*Year*	*Obs. Code*	*Star*
Bohlsen, T.	2016	BHQ	RZ Cha
Dvorak, S.	2008	DKS	FT Ori
Porio, J.	2016	PJTA	AI Hya
Samolyk, G.	2020	SAH	MY Cyg
Streamer, M.	2012	SFU	V526 Sgr
Vandenleve, M.	2012	VMAE	AG Per

TESS, KELT, and WASP (Butters *et al.* 2010) accessible from the NASA Exoplanet Archive (NASA 2023) and Hipparcos (Perryman *et al.* 1997). For convenience, reference hereafter to these sources is by their commonly known names/acronyms.

Some times of published minimum light photometry recorded portions of an eclipse in a phase range judged adequate (with caveats) for the present purpose where the fitted value of ω agreed with prediction.

It is noted that TESS observations are separately treated in single orbits. Limb darkening and gravity brightening coefficients for TESS data rely upon Claret (2017).

2.5. Fitting model

Uniform processing from a common model was implemented using BM3 (a Wilson-Devinney model) (Bradstreet and Steelman 2002), augmented with differential comparison facility.

Common reference data (absolute and orbital) are selected as noted above, from a published combined solution judged to exhibit least experimental uncertainties. Analysis, applied in common to the LCs of a given target, supports relative values and those relative uncertainties specific to the fitted inclination. The fixed reference parameters for absolute and orbital properties, e.g. other than i_c and ω, are then employed in the analysis of all LCs for the subject binary.

2.6. Uncertainty and weight

Weight is a measure of how a set of observations relate to a reference set of observations and the chosen model. This survey is directed to time dependence: weight is critical to that end and is determined as described in section 2.1.

It is unfortunate that the word "uncertainty" is common to several instances as noted below. Context should be considered where the term appears. Distinguish uncertainties in i_c (a relative parameter) from uncertainties of the physical parameter i. The latter uncertainty will appear in that cited publication, here selected as the zeroth orbit.

Uncertainty of the relative parameter value i_c, in tables and error bars, is derived from co-variance matrices of the (commonly employed) differential comparison procedure of the fitted parameter. Uncertainties in i_c result from operations establishing relationship with the reference parameters. These analytical uncertainties (often smaller than graph symbols) apply to the time-dependent behavior of inclination and are distinguished from the much larger physical/practical range of uncertainty applicable to inclination value.

Each binary considered here is represented by several LCs often regarded as occupying overlapping zones of physical absolute uncertainty. Parameter uncertainties herein are analytical, the better to illuminate comparison. An example is to be seen in Figure 9, where an evident trend in time dependence of i_c (upper panel) is compared with the classically determined values of inclination over the same interval (lower panel).

The regression coefficient will be quite sensitive to the relative weights. The present method is adopted with the goal of detecting subtle systematic trends of inclination (or not). Reliable relative weights and reliable relative inclination values are critical to that end.

2.7. Plots and tables

Observations in U or u light were often acquired concurrently with longer wavelength observations. These LCs are not included in the regression calculations and are not displayed in figures (with few exceptions).

Specific plotted data points may be identified from apparent figure coordinates and the associated table.

Table values for i_c and associated analytic uncertainty are rounded in the second decimal place (with some exceptions). Smin is usually rounded in the sixth decimal place.

3. Results

3.1. Eccentric orbit detached binaries

Binaries exhibiting no-zero eccentricity are treated separately.

3.1.1. α CrB

Photometry of Kron and Gordon (1953), re-analyzed together with spectroscopic data by Tomkin and Popper (1986), was taken as reference data. Earlier photometry from Stebbins (1928) provides primary eclipse data amid out-of-eclipse scatter. (His published normals were used here.) Volkov (2005) published analysis of more recent observations without observational log required for present use. Hipparcos observations, ASAS3 photometry, and x-ray observation of secondary eclipse by Schmitt (1998) are insufficient for the present study. A single orbit from TESS was limited for the present analysis to exclude much of one of the out-of-eclipse regions. Tomkin and Popper (1986) found rotation parameters F1 and F2 set to 4.07 and 1, respectively, for median orbital velocities. Schmitt *et al.* (2016) is notable for examination of apsidal motion in this system.

Table 2 collects the details of this analysis. Figure 1 includes the WLR; see Table 14. The entire orientation study spanning over 90 years shows apparently less than 0.2o variation. With only three discrete epochs available, the fit is tentative at best. This isolated binary merits further investigation.

This eccentric binary (e~.37) has been treated by Plavek (1960) and by Alexander (1976). Precession-associated nutation has been calculated. Plavek's estimate of such nutation period was 312.7 years (6602 orbits). Considering only precession-associated nutation, Alexander found a period for such nutation of 1780 orbits with semi-amplitude of 0.1degree (see Figure 6 of Alexander 1976). With no more than three data points, spanning the 2078-orbit study interval, that interval constitutes about 1.6 times the nutational period from Alexander. On that

Table 2. α CrB over 2078 orbits.

Orbit	i_c°	±	S_{min}	*RJD*	*Reference (λ)*
–547	87.98	0.04	0.007523	222894	1 (4500)
0	87.98	0.01	0.007767	32395	2; 3 (7230)
1531	88.13	0.0006	0.001496	58969	4 (I) truncated

References: 1. Stebbins (1928); 2. Kron and Gordon (1953); 3. Tomkin and Popper (1986); 4. TESS.

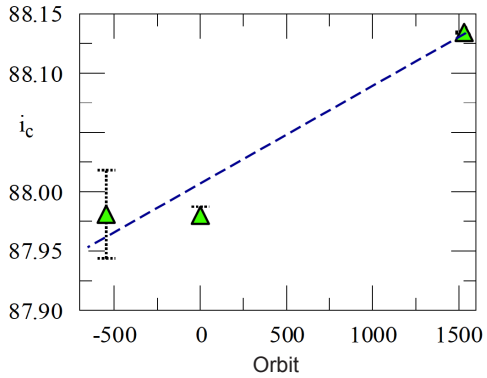

Figure 1. Orbital dependence of inclination for α CrB. Dashed line is WLR (see Table 14).

Table 3. V526 Sgr over 10787 orbits.

Orbit	i_c°	±	S_{min}	*RJD*	*Reference (λ)*
–10437	87.07	0.08	0.077876	27804	6 phg excluded
–5138	89.10	0.009	0.045282	37974	1 (B)
–5138	89.02	0.04	0.010699	37974	1 (V)
0	89.41	0.01	0.006868	47836	2 (B)
0	88.46	0.03	0.006277	47836	2 (V)
2928	88.17	0.01	0.0260835	53455	3 (V)
4346	87.67	0.01	0.004172	56178	4 (V)
5640	86.70	0.007	0.004781	58657	5 (I) truncated
5649	86.45	0.03	0.0055843	58679	5 (I) truncated

References: 1. O'Connell (1967); 2. Lacy (1993, 1997); 3. ASAS3; 4. Streamer (Kloppenborg 2023); 5. TESS (2023); 6. O'Connell (1935).

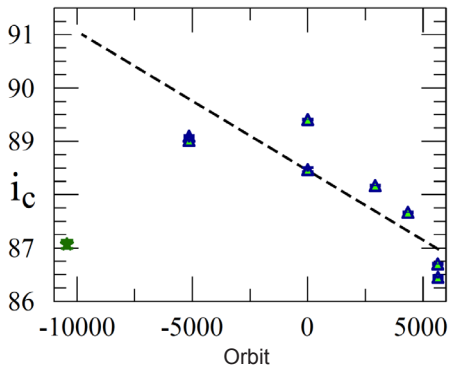

Figure 2. Orbital dependence of inclination for V526 Sgr. Dashed line is WLR (see Table 14). Star is O'Connell (1935).

basis, nutation would have progressed by 0.2° (one full period) in one direction and regressed by approximately 0.12° (0.6 period), with a net change of 0.17° over that interval. The present archival analysis yields a net difference of 0.15°. Uncertainties in both data and theoretical treatment aside, that result is consistent with Alexander (1976), which is meant to apply on a precession time scale.

3.1.2. V526 Sgr

Reference data were acquired and analyzed by Lacy (1993). Rotational parameters F1 and F2 (2.2 and 1.8) were found by Lacy (1997). Additional LCs were published by O'Connell (1967), by Streamer (Kloppenborg 2023), and from ASAS3. Both O'Connell and Lacy included significant third light, L_3, in analysis and the source of that light was separately studied by both authors. In the present work L_3 is consistently treated for all LCs from the reference solution. A photo LC from O'Connell (1935) is of interest relative to the extrapolated WLR established from photometric observations. Also see O'Connell (1948).

ASAS3 data were limited to the highest grade identified by the ASAS pipeline and obvious outliers were manually removed. TESS observations were separately analyzed from first and last single orbits recorded. These were cover the phase interval from 0.5 to 1.1 and were truncated elsewhere.

It is worth remarking that effects of precession-associated nutation (with a likely period of the order of a thousand orbits) contribute to deviations from the WLR line.

Table 3 collects the details of this analysis as shown in Figure 2. A dashed line represents the WLR; see Table 14 for details.

3.1.3. QX Car

The selected reference data set is Andersen *et al.* (1982, 1983) in b, y, and v (u excluded here). Those reference data were reduced by those authors in WINK, a model featuring triaxial geometry. Re-analysis in WD spherical geometry has been employed here. Rotational parameters F1 and F2 (2.2, 1.82) are supported from those authors' determinations.

Earlier observations were reported by Cousins (1981). To reduce artifact from apsidal motion, LC observations of Cousins *et al.* (1981) in V were here limited to 2440344 < HJD > 2440703 (avoiding a lengthy gap). The LCs from Hipparcos and ASAS3 are of similar phase coverage to Cousins and to Anderson *et al.* For data from the ASAS3 project, obvious outliers were manually deleted. No indications of third body influence were noted by any of these authors.

Gimenez *et al.* (1986b) contributed further observations of eclipse II in apsidal motion studies (not used herein). KELT (east) data are excluded from WLR analysis. (The out-of-eclipse observations are excessively scattered and only the approximate upper half of both eclipses is recorded.) Each of the earliest and latest full orbits from TESS have been separately treated.

No evidence of third body perturbation has been reported.

Table 4 contains the detail of this analysis as presented in Figure 3. A dashed line represents WLR; see Table 14 for details.

3.1.4. AR Cas

The reference data set for the present work was based on the WD fit to photometry of Catalano and Rodono (1971) combined

Table 4. QX Car over 3091 orbits.

Orbit	i_c °	±	S_{min}	*RJD*	*Reference (λ)*
–795	85.82	0.06	0.01039	40010	1 (B)
–643	85.64	0.01	0.011503	40692	1 (V) truncated
0	85.82	0.02	0.004846	43572	2 (y)
0	85.80	0.05	0.00342	43572	2 (v)
0	85.82	0.05	0.004830	43572	2 (b)
1094	85.24	0.12	0.016996	48471	3 (H_p)
2296	85.55	0.04	0.018749	53853	4 (V)
3509	85.16	0.02	0.003296	59287	5 (I)
3512	85.12	0.02	0.003614	59302	5 (I)

References: 1. Cousins (1981); 2. Andersen et al. (1982); 3. Hipparcos; 4. ASAS3; 5. TESS.

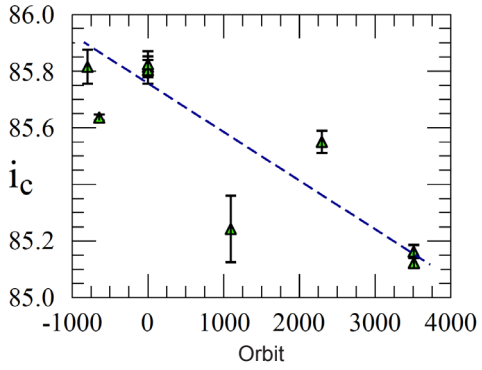

Figure 3. Orbital dependence of inclination for QX Car. Dashed line is WLR (see Table 14).

Table 5. AR Cas over 6063 orbits.

Orbit	i_c °	±	S_{min}	*RJD*	*Reference (λ)*
–2987	85.36	0.06	0.013953	22005	1 (4500)
–1259	83.88	0.07	0.011744	32490	5 (4200) primary
–1231	85.28	0.11	0.010257	32656	2 (B)
–780	84.83	0.01	0.006861	35396	4 (5400)
–780	84.28	0.07	0.006715	35396	4 (4200)
–535	83.82	0.1	0.017484	36882	5 (V)
–535	83.83	0.21	0.011955	36882	5 (B)
–535	84.32	0.27	0.017230	36882	5 (G)
–535	85.63	0.14	0.0168266	36882	5 (R)
–535	84.61	0.22	0.016026	36882	5 (I)
0	83.81	0.17	0.037639	40126	3 (V)
0	84.11	0.19	0.00515816	40126	3 (B)
1092	85.36	0.38	0.0309811	46750	6 (V) secondary
1806	84.36	0.2	0.011711	51084	7 (V) primary
3073	85.26	0.01	0.004452	58768	8 (I)
3076	85.19	0.003	0.004436	58786	8 (I)

References:1. Stebbins (1921); 2. Botsula and Kostylev (1960); 3. Catalano and Rodono (1971); 4. Huffer and Collins (1962); 5. Gordon and Kron (1973); 6. Mossakovskaya (1992); 7. Holmgren et al. *(1999); 8. TESS.*

with spectroscopic results from Holmgren *et al.* (1999). The final 14 points of the observations of Catalano and Rodono (1971) were truncated in the present work to avoid a year gap in the data record. The photometry of Holmgren *et al.* (1999) was limited to data from San Pedro Martir and Hvar, a combination of observations which utilized the same comparison star, were acquired in a narrow time interval, and were directed to the primary eclipse. Holmgren *et al.* (1999) determined F1 as 3.0 and F2 was assumed pseudosynchronous.

Photoelectric observations for the present study included Botsula and Kostylev (1960) and Mossakovskaya (1992), the latter limited to eclipse II. The discovery work of Stebbins (1921) is treated here, with magnitude corrections per Holmgren *et al.* (1999). The observations of Gordon and Kron (1973) present primary eclipse data adequate for present purposes. Hipparcos data were insufficient for present use.

TESS observations were limited to single orbits, separately analyzed. Information content of such orbits is effected by a pulsating component which is ignored in present study. An approximately 0.25-φ phase region of one out-of-eclipse phase interval was truncated.

The observations of Huffer and Collins (1962) covering the primary eclipse phase interval 0–0.032 Φ (at 420 and 540 microns) are included here with caveats. These data were published only by phase. For present use essential chronology is estimated from a fitted value of ω.

Figure 4 is distinguished from many such of this study by the wide scatter of relative inclination over the study interval. Replacing concurrently acquired data with weighted averages of concurrent points and simple average of uncertainties does not reveal a trend, but the result is not inconsistent with the several tenths degree amplitude and thousands orbits period expected for precession-associated nutation. Orbital data is given in Table 5. The WLR parameters are formally included in Table 14.

Note that from consistent solutions with constant e for three LCs including their own, Holmgren *et al.* (1999) found a decreasing inclination over about 80 years in contrast to present weighted WLR for relative inclination. Krylov *et al.* (2003) also performed consistent solutions for 10 LCs reviewed over this period. With no constraint on e, those analyses exhibit no specific trend.

For AR Cas, systemic velocity differences discussed by various workers and other indicia of possible third body presence were considered and rejected by Holmgren *et al.* (1999). Krylov *et al.* (2003) determined substantial L_3 and identified AR Cas with visual multiple ADS 16795 with no estimated P_3.

3.1.5. FT Ori

Light curves of FT Ori acquired at widely spaced epochs were reported and analyzed by Sabby *et al.* (2011). These data included B and V light curves and radial velocities acquired at CTIO by co-author Lacy, circa 1993–1995; light curves acquired at Ege by co-author Ibanoglu in 1972; and by Cristaldi at Catania in 1963–1965 (see Cristaldi 1970). Later LCs have been acquired from ASAS3, the SWASP survey, and (eclipse II) by Dvorak (Kloppenborg 2023).

Sabby *et al.* (2011) reported a consistent treatment of five LCs from three separate epochs using common values for the mass ratio q and gravity brightening. Although Cristaldi's LC was observed in 1513 observations, that LC was only published in normal points (his observation logs are inaccessible). Textual clues and fitted value for ω provide the RJD displacement.

In the 80-year record for times of minimum light for FT Ori, Sabby *et al.* (2011) remarks that no anomalies appear suggesting a third body.

Table 6. FT Ori over 5254 orbits.

Orbit	i_c°	±	S_{min}	*RJD*	*Reference (λ)*
-3624	88.77	0.12	0.006730	38478	1 (BG)
-2598	89.91	0.29	0.008991	41663	2 (B)
-2598	89.62	0.34	0.009172	41663	2 (V)
0	90.05	0.04	0.000900	49731	2 (B)
0	90.01	0.013	0.005447	49731	2 (V)
1280	90.36	0.28	0.0481166	53704	5 (V)
1468	90.15	0.01	0.017650	54288	3 (V)
1509	90.15	0.01	0.01760	54416	6 (R)
1630	89.97	0.02	0.00518	54791	4 (V) secondary

References: 1. Cristaldi (1970); 2. Sabby et al. *(2011); 3. WASP; 4. Dvorak (Kloppenborg 2023); 5. ASAS3; 6. KELT (east).*

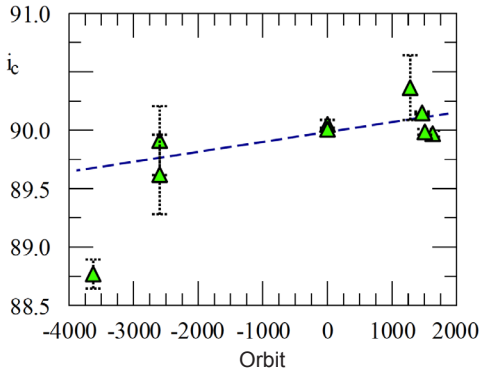

Figure 5. Orbital dependence of inclination for FT Ori. Dashed line is WLR (see Table 14).

Orbital dependence of inclination for FT Ori is shown in Figure 5; Orbit data is given in Table 6.

3.1.6. V346 Cen

Gimenez *et al.* (1986a) is selected as the reference parameter set. Mayer *et al.* (2016) have particularly studied a spontaneous change in period at about HJD 2439000, prior to available photometric LCs. These authors found no explanation for the abrupt change in orbital period. No evidence for a third body was found in either photometric or spectroscopic data. Prior to the reference observations, LCs were acquired by van Houten *et al.* (2009). These data, sparse, available only by phase, and calibrated by various comparison stars, yield i_c values far above others and are excluded from WLR. Additional observations were obtained from ASAS3 and KELT (east). The latter is plotted for the record but excluded from the WLR analysis. (KELT observations are excessively smeared in magnitude in out-of-eclipse regions.)

Mayer *et al.* (2016) combined their own observations with the Hipparcos LC and separately included LCs from several other facilities for their analysis. Their spectroscopic observations included rotation parameters 2.418 and 2.805 for F1 and F2, respectively. They also reconstructed photographic observations of O'Connell (1939), which are separately processed herein although excluded from WLR fitting operation. O'Connell's photographic LC (not shown in Figure 6) with analytic uncertainty ~0.1° produces an i_c value about 2° above the WLR trend line at –2700 orbits. The epoch of O'Connell's photo LC is most proximate the apparent discontinuity in sidereal period. See Figure 2 noted of Mayer *et al.* (2016).

Table 7. V346 Cen over2326 orbits.

Orbit	i_c°	±	S_{min}	*RJD*	*Reference (λ)*
–2696	86.81	14.2	0.020027	42178	6 phg excluded
–444	85.51	0.05	0.020437	42178	5 (B) excluded
–444	85.51	0.14	0.02046	42178	5 (V) excluded
0	83.95	0.006	0.005578	45117	1 (v)
0	84.34	0.003	0.009610	45117	1 (b)
0	83.98	0.01	0.005387	45117	1 (y)
1351	84.00	0.02	0.012300	53660	3 (V)
1629	84.91	0.05	0.014646	56755	2 (B)
1629	84.66	0.05	0.014104	56755	2 (V)
1629	85.55	0.08	0.013087	56755	2 (R)
1841	84.60	0.01	0.023189	55418	2 (B)
1841	84.28	0.01	0.011318	55418	2 (V)
1841	84.36	0.01	0.014206	55418	2 (R)
1842	84.38	0.01	0.014239	56765	2 (I)
1882	82.87	0.02	0.013535	57016	4 (R) excluded

References: 1. Gimenez et al. *(1986a); 2. Mayer* et al. *(2016); 3. ASAS3; 4. KELT (east); 5. Van Houten et al. (2009); 6. O'Connell (1939)*

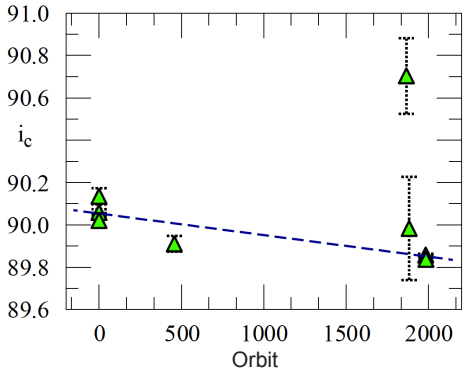

Figure 6. Orbital dependence of inclination for V346 Cen. Dashed line is linear regression (see Table 14 for detail). Star is excluded KELT datum.

The content of Table 7 appears in Figure 6. A dashed line represents the WLR (starred points excluded); see Table 14 for detail.

3.1.7. AI Hya

The most extensive observations were acquired by Jørgensen and Grønbech (1978) in uvby and analyzed by Popper (1988). These data comprise the reference data set. F1 and F2 were assumed pseudosynchronized. The observations of Khaliullin and Kozyreva (1989) in V-filter cover phase regions of primary descending arm and secondary ascending arm of both eclipses. A sparse (72-point) LC covering the full phase region is recorded by Porio (Kloppenborg 2023). A full phase LC is obtained from the ASAS-SN project (Shappee *et al.* 2014). TESS observations were binned over four consecutive observations with appropriate phase correction. First and last full (binned) orbits were independently analyzed. Recent TESS photometry analysis of Lee *et al.* (2020) is of interest.

A photographic LC (orbit number –1585) from Lause (1938), excluded from both fitting and Figure 7, yields i_c value 2° higher than back-extrapolated WLR.

Table 8 collects the details of this analysis. A dashed line represents the WLR; see Table 14 for detail.

Table 8. AI Hya over 1983 orbits.

Orbit	i_c °	±	S_{min}	RJD	Reference (λ)
–1585	91.88	0.042	0.04735	28935	phtg excluded
0	90.13	0.04	0.015219	42072	1; 2 (v)
0	90.06	0.01	0.013453	42072	1; 2 (b)
0	90.02	0.03	0.013865	42072	1; 2 (y)
458	89.91	0.04	0.01405	45868	3 (V)
1865	90.70	0.2	0.039223	57532	4 (V)
1882	89.98	0.24	0.043020	57675	5 (V)
1982	89.86	0.005	0.08068	58506	6 (I) truncated
1983	89.84	0.008	0.011749	58517	6 (I) truncated

References: 1. Jørgensen and Grønbech (1978); 2. Popper (1988); 3. Khaliullin and Kozyreva (1989); 4. Porio (Kloppenborg 2023); 5. ASAS-SN; 6. TESS.

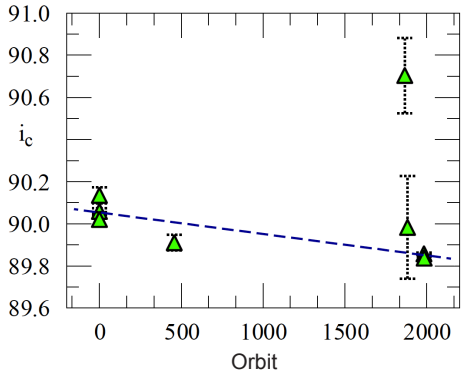

Figure 7. Orbital dependence of inclination for AI Hya. Dashed line is WLR (see Table 14).

3.1.8. AG Per

AG Per has been identified with the Per OB2 association by Gimenez and Clausen (1994) and others, and assumed by them to form a triple system with ADS 2990 B on the basis of similar orbital observations. No period (P_3) is suggested by them for a bound triple (for which reason AG Per is here included).

The analysis by Gimenez and Clausen (1994) of the LCs published by Güdür (1978) was selected as reference data set. Constituent rotations were taken as pseudosynchronized. Together with that reference, the LCs of Huffer (1928), Ashbrook (1949), Jones (1969), Semeniuk (1968), Gimenez *et al.* (1987), and the Hipparcos mission provide distinct LC epochs. Woodward and Koch (1987) published by phase but provided a suitable time datum. The Huffer LC has been scrutinized with no evident unusual properties accounting for i_c outside the fitted trend in ω. A photographic LC from Martin (1938) is of interest but excluded from WLR fitting.

The most recent photometry by Vandenleve (Kloppenborg 2023) comprises single orbit (CCD) observations of the full secondary eclipse. These observations were divided into earlier and later portions. In satisfactory mutual agreement and carrying heavy statistical weighting but yielding unaccountably high i_c value, these are provisionally excluded from WLR analysis to preserve the character of the earlier data for separate analysis. Further data are anticipated with interest.

The behavior of orientation for AG Per over nearly fifteen thousand orbits is consistent with perturbation from an aperiodic and perhaps nearly constant companion. The status of AG Per as isolate or triple is unresolved.

Table 9. AG Per over 15059 orbits.

Orbit	i_c °	±	S_{min}	RJD	Reference (λ)
–8716	81.42	0.04	0.013483	225038	1 (4500)
–6785	80.71	0.04	0.030706	228955	11 pht excluded
–4823	81.25	0.03	0.008104	332935	2 (~4500)
–2334	81.51	0.06	0.015983	337984	6 (V)
–2334	81.62	0.08	0.016887	337984	6 (B)
–2150	81.27	0.03	0.006137	338358	3 (Y)
–192	81.51	0.02	0.006791	442330	7 (b)
–192	81.50	0.02	0.007157	442330	7 (y)
0	81.38	0.04	0.006542	442720	4; 5 (B)
0	81.35	0.01	0.005121	442720	4; 5 (V)
1079	81.40	0.06	0.009055	444908	10 (V)
1079	81.44	0.04	0.007343	444908	10 (B)
2846	81.67	0.29	0.020451	448494	8 (H_p)
5783	82.68	0.01	0.012920	554452	9 (V) secondary, excluded
6343	82.50	0.01	0.027083	55590	9 (V) secondary, excluded

References: 1. Huffer (1928); 2. Ashbrook (1949); 3. Semeniuk (1968); 4. Güdür (1978); 5. Gimenez and Clausen; (1994); 6. Jones (1969); 7. Woodward and Koch (1987); 8. Hipparcos; 9. Vandenleve (Kloppenborg 2023); 10. Gimenez et al. (1987); 11. Martin (1938).

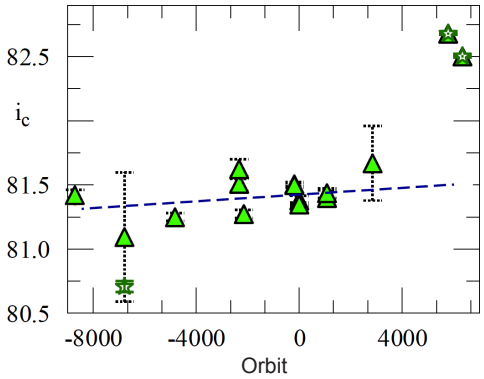

Figure 8. Orbital dependence of inclination for AG Per. Dashed line is WLR (see Table 14). Stars are excluded from WLR.

Plavek (1960), following Kopal (1959), estimated a period of 268.5 years (43358.5 orbits or 1.14e-4 °/orb) for Kopal's "P10" period. In contrast, Alexander (1973) treated the long-term evolving nature of AG Per, ignoring the precession-associated nutation (Plavek 1960), whereas the empirical rate (found here) necessarily is an average of combined evolving inclination as well as precession-associated nutation. Table 9 collects the details of this analysis. The time dependence of i_c for AG Per as obtained herein is shown in Figure 8.

3.2. Circular Orbit (Isolate) Detached Binaries

The following binaries with eccentricities less than 0.01 and nearly synchronized constituent rotations are considered separately. Precession with associated nutation will approach a null as e approaches 0 and synchronization is realized. If not fully circular and synchronized, remnant precession effect, although greatly attenuated, may yet be present.

3.2.1. YZ Cas

This circular orbit, detached binary has been photometricaly observed over six decades. For the present study, the selected reference parameter set is Kron (1942) from the Pavlovski *et al.* (2014) re-analysis. For the present work e is set to 0.001,

a value within uncertainties stated by Pavlovski *et al.* (2014) and also by Lacy (1981). The present study includes Diethelm and Lines (1986; in Breger 1988) and Huffer (1928), which were inadequate for the purposes (absolute properties) of Pavlovski *et al.* Certain phased LCs referenced by the latter were unavailable to the present study.

Selected single orbit LCs from the TESS mission were separately analyzed. Truncation consisted of the excise of one out-of-eclipse region while retaining the other.

The present work (Figure 9, upper panel, with triangle points and relative error bars) suggests a slightly negatively weighted orientation with nearly equal magnitude uncertainty. No third body anomalies appear in the literature.

Table 10 collects the details of the present analysis as shown in Figure 9 (upper panel). A dashed line represents the WLR over 7863 orbits; see Table 14 for detail.

Pavlovski *et al.* (2014) independently examined each of 15 LCs to obtain solutions (uniformly, using jktebop (Southworth *et al.* (2004)) in the classic manner (Figure 9, lower panel). Treated in identical fashion (relative to reference parameters), those inclinations, assigned RJD centroid dates per this work (or approximated from textual clues), are shown in Figure 9 (lower panel), on identical scale of ordinate and abscissa. Those results, weighted herein by Pavlovski's inverse squared uncertainties, yield a WLR coefficient $-9.9 \times 10^{-5} \pm 6.2 \times 10^{-5}$ °/orbit. The uncertainties published from Pavlovski *et al.* (2014) represent physical uncertainties; e.g. uncertainties from a Monte Carlo procedure providing weights for comparison with present work (–3.9e–5 ± 1.6e–5 °/orbit).

Lacy (1981) determined v_1 sin i as 20% in excess over orbital velocity and v_2 sin I synchronized. A broad interpretation of the trend of inclination of Figure 9 suggests a continued approach to orbital alignment as described by Hut (1981).

3.2.2. β Aur

This (nearly) circular orbit, rotationally synchronized binary has been widely studied. Southworth *et al.* (2007) is selected as reference data, notably precise in analysis of WIRE satellite photometry. Johansen (1971) contributed eight LCs, the more numerous and earliest included herein, and Nordstrom and Johansen (1994) added analysis. Hipparcos observations are of notable quality. Historic observations (Stebbins 1911), with a selenium cell, are noteworthy in this relative context. A number of spectroscopic observations include Popper and Carlos (1970) and citations therein.

Southworth *et al.* (2007) find a non-vanishing eccentricity of 0.00183 and $v_{synch\,1,2}$ values 35.3, 32.8 km/s, both ±0.2, suggesting that circularization and synchronization are not fully realized; thus, some remnant precession-associated nutation might be expected. The (standard error) uncertainty in the WLR coefficient is about 3.2 times the derived value; there is some justification for interpreting this as representation of accumulated uncertainties. That suggests the precession-associated nutation is null and the orbital axis of this nearly circular synchronous orbit to be fully aligned with the constituent rotational axes (undetectable change in inclination rate).

Table 11 collects results of this analysis. Figure 10 displays those results with dashed line representing the inverse S_{min} weighted WLR; see Table 13a for detail.

Table 10. YZ Cas over 7857 orbits.

Orbit	i_c °	±	S_{min}	*RJD*	*Reference (λ)*
–1304	88.85	0.08	0.013544	23863	1 (4500)
–ß160	88.70	0.01	0.007469	28971	1 (4500)
0	88.38	0.01	0.009002	29687	3 (6000)
787	88.91	0.01	0.009354	33201	4 (3575)
787	88.50	0.01	0.009364	33201	4 (4525)
3390	88.76	0.01	0.013329	44832	5 (4720)
3390	88.50	0.03	0.013557	44832	5 (6720)
3390	88.50	0.03	0.013416	44832	5 (7810)
3390	88.59	0.02	0.013095	44832	5 (8710
3604	88.44	0.02	0.0156	45787	6 (V)
3604	88.55	0.04	0.017823	45787	6 (B)
4163	88.79	0.09	0.006389	48283	7 (H_p)
6553	88.85	0.002	0.002704	59007	8 truncated
6559	88.90	0.002	0.001786	58986	8 truncated

References: 1. Huffer (1928); 2. Kron (1939); 3. Kron (1942); 4. McNamara (1951); 5. Provoost (1980); 6. Breger (1988); 7. Hipparcos; 8. TESS.

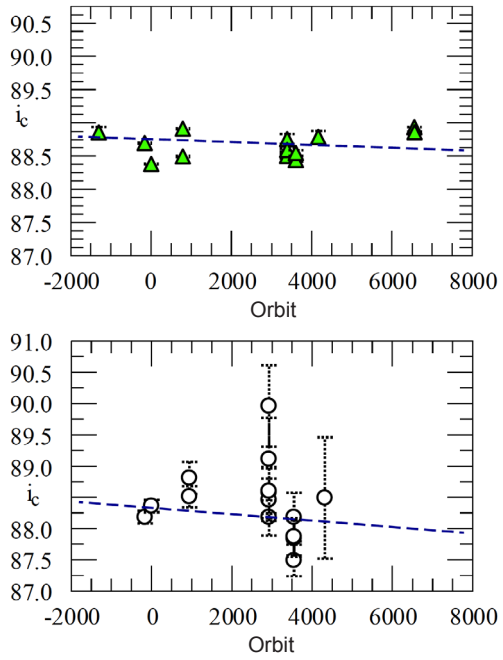

Figure 9. Upper pannel, this work. Dashed line is WLR (Table 14 for detail). Lower panel, Pavlovski *et al.* (2014) identical scales.

3.2.3. MY Cyg

This nearly circular orbit (e ~ 0.01) exhibits significant apsidal motion and has been studied in some detail. The LCs of Williamon (1975) are selected with analysis of Tucker *et al.* (2009) as reference. Additional LCs from Tremko *et al.* (1978), Hipparcos, Coughlin (see Tucker *et al.* 2009), Samolyk (Kloppenborg 2023), and TESS are here treated. Rotation was assumed pseudosynchronized per Tucker *et al.*

Observations of Coughlin principally comprise descending eclipse arms with a few points of ascending arms. These observations were excluded from analysis by Tucker *et al.* (2009) and similarly herein (but shown in Figure 11). Tremko *et al.* (1978) published separate observing campaigns at Skalnate Pleso and Brno University Observatories, nearly overlapping in time. Their V observations (Skalnate Pleso) are here truncated in time to those earlier than RJD 39056 to

Table 11. β Aur over 8787 orbits.

Orbit	i_c°	±	S_{min}	*RJD*	*Reference (λ)*
–8787	76.98	0.13	.00915	19038	1 (unfiltered)
–4180	76.60	0.01	.006917	37284	2 (B)
–4084	77.21	0.07	.012526	37661	2 (V)
–3688	77.01	0.06	.009345	39229	2 (vf)
–3688	77.02	0.05	.084603	39229	2 (yf)
–3688	76.95	0.06	.006793	39229	2 (bf)
–1346	76.67	0.1	.003729	48504	3 (H_p)
0	76.94	0.002	.003116	53836	4 (V+R)

References: 1. Stebbins (1911); 2. Johansen (1971); 3. Hipparcos; 4. Southworth et al. *(2007).*

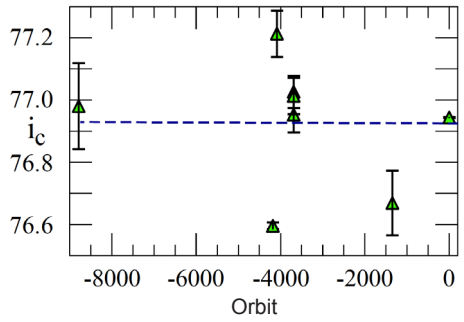

Figure 10. Orbital dependence of inclination of β Aur. Dashed line is WLR (see Table 14).

Table 12. MY Cyg over 5324 orbits.

Orbit	i_c°	±	S_{min}	*RJD*	*Reference (λ)*
–883	88.56	0.01	0.020227	38679	6 (V) secondary
–312	88.59	0.030218158		40764	6 (B)
0	88.72	0.01	0.016532	42019	1 (B)
0	88.55	0.02	0.015568	42019	1 (V)
1599	88.72	0.09	0.017217	48431	2 (H_p)
2997	88.47	0.02	0.013698	54032	3 (V) excluded
2997	89.63	0.09	0.017097	54032	3 (B) excluded
2997	90.00	0.19	0.017368	54032	3 (R) excluded
2997	88.74	0.03	0.014899	54032	3 (I) excluded
4279	88.67	0.01	0.006908	59173	4 (V)
4435	88.49	0.001	0.003014	59799	5 (I)
4441	88.48	0.001	0.003199	59822	5 (I)

References: 1. Tucker et al. *(2009); 2. Hipparcos; 3. Coughlin (2007; see 1); 4. Samolyk (Kloppenborg 2023); 5. TESS; 6. Tremko* et al. *(1978).*

obtain the earliest i_c (limited to eclipse II). The B observations (Skalnate Pleso) are treated in full phase coverage. Hipparcos observations comprise 5 points in primary and 12 points in secondary eclipse with appropriate weighting herein.

From Figure 11 one is tempted to interpret superficially the inclination rate as flat over the study period to the contrary of the WLR coefficient. Tucker *et al.* (2009) found non-vanishing e and significant apsidal motion. Lacking spectroscopic study, a state of synchrony is not established. An evolving state apparently continues. Orbital data are given in Table 12.

3.2.4. RZ Cha

This apparently circular synchronous binary was the subject of definitive LC photometry by Jørgensen and Gyldkenkerne (1975) and spectral study by Andersen *et al.* (1975), with

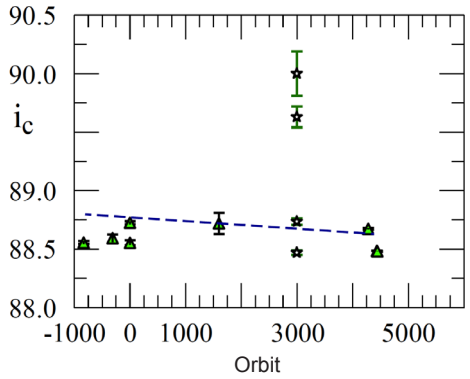

Figure 11. Orbital dependence of inclination for MY Cyg. Dashed line is WLR (see Table 14). Stars are excluded.

Table 13a. RZ Cha over 6595 orbits.

Orbit	i_c°	±	S_{min}	*RJD*	*Reference (λ)*
0	82.54	0.01	0.009665	41446	1 (y)
0	82.43	0.01	0.00781	41446	1 (b)
0	82.45	0.01	0.0087227	41446	1 (v)
1057.1	83.37	0.06	0.008086	44440	2 (V) primary
2457.5	83.20	0.07	0.01542	48406	3 (H_p)
3060.9	82.36	0.01	0.022837	50115	4 (V)
5679.2	83.08	0.002	0.013338	57530	5 (V) primary
6586.3	83.11	0.003	0.001742	60099	6 (I)
6594.7	83.14	0.005	0.001665	60123	6 (I)

References: 1. Jørgensen and Gyldenkrne (1975); 2. Mallama (1981); 3. Hipparcos; 4. ASAS3; 5. Bohlsen (Kloppenborg 2023); 6. TESS.

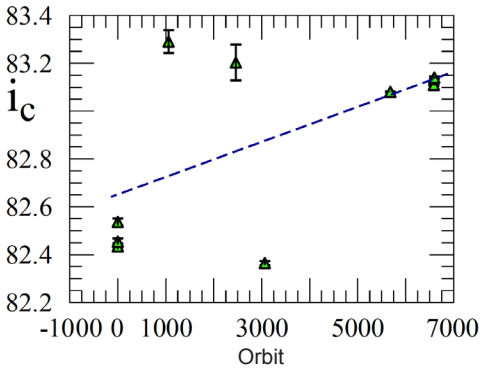

Figure. 12. Orbital dependence of inclination of RZ Cha. Dashed line is WLR (see Table 14).

Table 13b. Selected WD parameters for RZ Cha.

Parameter	*Value*	*Unit*
r_1	0.1897	separation of stellar centers
r_2	0.1782	separation of stellar centers
i_c	83.099	degrees

reanalysis by Giuricin *et al.* (1980) using WINK. For consistency the present work required further analysis in a WD model for the set of reference parameters. The LCs in y, b, and v were so analyzed, and weighted averages for r_1, r_2, and i_c appear in Table 13b. Additional photometry from Hipparcos, Kloppenborg (2023), ASA3, Mallama (1981), and TESS complete known observations.

Synchrony was concluded from observation by Andersen *et al.* (1975). No measure of eccentricity appears in the literature. The present study employs a nominal eccentricity of 0.001.

RZ Cha may represent a fully synchronous circular orbit binary; thus, the WLR is notable as representing an inclination rate similar to YZ Cas and MY Cyg, not so fully synchronous and circular. That is, progress continues for alignment of the rotational axes of RZ Cha. Complete alignment is as characteristic of the evolved state as circular synchronicity; RZ Cha continues to align.

Table 14. WLR summary.

System	*Δi*	± *°/orbit*	*Intercept (°) °/orbit*
α CrB	8.23×10^{-5}	1.5×10^{-5}	88.007 ± 0.020
V526 Sgr	-2.61×10^{-4}	6.2×10^{-5}	88.0825 ± 0.278
AR Cas	1.22×10^{-4}	7.9×10^{-5}	84.639 ± 0.147
FT Ori	8.46×10^{-5}	4.1×10^{-5}	89.984 ± 0.050
V346 Cen	2.72×10^{-4}	1.7×10^{-4}	84.117 ± 0.235
QX Car	-1.72×10^{-4}	1.6×10^{-5}	85.653 ± 0 .042
AI Hya	1.52×10^{-4}	1.5×10^{-5}	9ß0.003 ± 0.144
AG Per	2.37×10^{-5}	1.3×10^{-5}	81.442 ± 0.045
Near circular, synchronous:			
YZ Cas	–3.91 × 10-5	1.6 × 10-5	88.598 ± 0.075
MY Cyg	–2.3 × 10-5	1.6 × 10-5	88.625 ± 0.063
Œ≤ Aur	7.90 × 10-6	2.5 × 10-5	76.923 ± 0.052
RZ Cha	7.33 × 10-5	2.7 × 10-5	82.652 ± 0.148

4. Discussion

Table 14 summarizes the WLR fits of the present work. In respect to line of sight, a negative coefficient distinguishes the sense of rotation of the orbital plane about an axis in that plane (approach and recession from line-of-sight) and may be ignored. A parallel study of triple structures (in progress) tends to show corresponding orientation variation five to ten times greater, as expected, where the tertiary perturbation is a controlling factor.

4.1. Time scales: long and short

Hut (1981) has treated evolution of orbital elements of a binary constituent on an evolutionary time scale (Myr), invoking a tidal time lag in a tidal friction model. In practice that time scale is long compared to sub-periods of precession periods examined by Alexander (1976), e.g. a short time scale. The present empirical results obviously relate to a combination of long and short term time scales. Three nearly circular synchronized binaries (YZ Cas, β Aur, and MY Cyg) are of particular interest approximating long time scale conditions as precession closely approaches a null. For a fourth such binary, RZ Cas, no evidence appears for departure from circular synchronicity. In his development of evolving parameters of rotating constituents, Hut (1981) averages over precession by ignoring the same. Consequently, the empirical determination of rate of change of orbital inclination for RZ Cha may approximately equate with the conditions of Hut's result (his Equation 13, explicitly derived as an average over an *orbit*) for rate of change of constituent misalignment. Hut's evolving "inclination," or *misalignment*, is the changing angle between the orbital plane and the equatorial plane of the primary. This (misalignment) inclination enters the expression for rate of change: an advanced stage of evolution is consistent with a choice of alignment angle A where Â is the determined rate of change for i_c. Assume that ΔA is identified with Δi_c.

As noted in section 3.2.2, β Aur, a nearly circular synchronous binary, can reasonably be considered to have closely reached a state of axial alignment.

Applying his work to AG Per, Alexander (1973) found a limit in that case for tidal lag as $\tau > 4.4\times10^{-2}$ sec. AG Per, with well-known eccentricity and apsidal motion, necessarily includes precessional effect with doubtful relevance of the present result to Hut.

Eccentric non-synchronous systems are treatable per Alexander (1973, 1976), an exercise presently postponed. One of Alexander's numeric results, α CrB, is briefly discussed in section 3.1.1. Consider that for any of the binaries here studied, the deviation of i_c from the WLR line reflects combined tidal friction evolution and expected precession-associated nutation as well as accumulated uncertainties. Compare these eccentric targets with deviations for nearly synchronous circular orbit binaries as noted above where precession-associated nutation is nearly negligible.

4.2. Inclination correction

As noted above, values of i_c are proxies from which a rate of change within or proximate the study interval is empirically determinable. It is urged that epochal displacement from the reference data set be applied to obtain a corrected inclination for any time appropriate to the study interval. Note that the uncertainty for the interpolated inclination value is to be drawn from the cited reference solution increased by the relative uncertainty for the RJD of the associated table.

4.3. Alternative hypotheses

(1) The evolutionary status of RZ Cha might be fully circular and synchronous within uncertainties. Absent a bound third body (assumed) and within a fully synchronous circular state (assumed), a non-vanishing orbital inclination rate suggests continued intrinsic contribution to non-apsidal rotation of the orbital plane. While three degrees of translatory motion (proper motion) of the center of mass are commonplace, three degrees of rotational motion remain to be considered (one of which is identified as apsidal motion). Within the above assumptions an intrinsic contribution to total angular momentum of the RZ Cha system might be contained within the present empirical inclination rate (Table 14). Any test of that hypothesis is problematic but isotropy of space suggests those degrees of rotational freedom are exercised.

(2) It is the absence of evidence of third body perturbation that suggests an isolate character for the targets of this survey.

The presently-demonstrated nutation trends might be explored as such evidence. The challenge is to determine independent evidence pointing to such hypothetical third body.

4.4. Miscellany

With regard for terrestrial observations, it is noted that the mean obliquity rate for earth is about 0.024 "/century Williams (1994), or about 0.6×10^{-7} °/year and not a significant correction for terrestrial photometric observations yielding i_c.

Finally, a traditional suggestion for more research is here taken for the identification and availability of data already in existence: observing logs, theses, unpublished dissertations, observatory publications and the more phase-extensive minimum light determinations. Data from past epochs are of the greatest value for any time-dependent phenomena.

5. Acknowledgements

This research has made use of the SIMBAD database and the VizieR catalogue access tool maintained by CDS, Strasbourg, France, for which the author is immensely grateful. The following internet-based resources were used in research for this paper: the NASA Astrophysics Data System; the arXiv scientific paper preprint service operated by Cornell University; the NASA Exoplanet Archive, operated by the California Institute of Technology, under contract with the National Aeronautics and Space Administration under the Exoplanet Exploration Program. I acknowledge with thanks the variable star observations from the AAVSO International Database contributed by observers worldwide and used in this research. The comments of the anonymous referee have contributed to a great extent in clarification of this work.

No public funds have been expended in support of this work.

References

Alexander, M. E. 1973, *Astrophys. Space Sci.*, **23**, 459.
Alexander, M. E. 1976, *Astrophys. Space Sci.*, **45**, 105.
Andersen, J., and Clausen, J. V. 1982, *Astron. Astrophys., Suppl. Ser.*, 49, 571.
Andersen, J., Clausen, J. V., and Nordstroem, B. 1983, *Astron. Astrophys.*, **121**, 271.
Andersen, J., Gjerloff, H., and Imbert, M. 1975, *Astron. Astrophys.*, **44**, 349.
Ashbrook, J. 1949, *Astron. J.*, **55**, 2.
Botsula, R. A., and Kostylev, K. V. 1960, *Bull. Astron. Obs. Kazan*, **35**, 34.
Bradstreet, D. H., and Steelman, D. P. 2002, *Bull. Amer. Astron. Soc.*, **34**, 1224.
Breger, M. 1988, *Publ. Astron. Soc. Pacific*, **100**, 751.
Butters, O. W., *et al.* 2010, *Astron. Astrophys.*, **520**, L10.
Catalano, S., and Rodonò, M. 1971, *Astron. J.*, **76**, 557.
Claret, A. 2017, *Astron. Astrophys.*, **600A**, 30.
Claret, A., and Gimenez, A. 1989, *Astron. Astrophys. Suppl. Ser.*, **81**, 1.
Claret, A., and Gimenez, A. 1990, *Astrophys. Space Sci.*, **169**, 215.
Coughlin, J. L. 2007, undergraduate thesis, Emory Univ., Atlanta, GA.
Cousins, A. W. J. 1981, *South Afr. Astron. Obs. Circ.*, **6**, 1.
Cristaldi, S. 1970, *Astron. Astrophys.*, **5**, 228.
Gimenez, A., and Clausen, J. V. 1994, *Astron. Astrophys.*, **291**, 795.
Gimenez, A., Clausen, J. V., and Andersen, J. 1986a, *Astron. Astrophys.*, **160**, 310.
Gimenez, A., Clausen, J. V., and Jensen, K. S. 1986b, *Astron. Astrophys.*, **159**, 157.
Gimenez, A., Kim, K. C.-H., and Nha, I.-S. 1987, *Mon. Not. Roy. Astron. Soc.*, **224**, 543.
Giuricin, G., Mardirossian, F., Mezzetti, M., and Predolin, F. 1980, *Astron. Astrophys.*, **85**, 259.
Gordon, K. C., and Kron, G. E. 1973, *Astrophys. Space Sci.*, **23**, 403.
Güdür, N. 1978, *Astrophys. Space Sci.*, **57**, 17.
Holmgren, D. E., Hadrava, P., Harmanec, P., Eenens, P., Corral, L. J., Yang, S., Ak, H., and Bozić, H. 1999, *Astron. Astrophys.*, **345**, 855.
Huffer, C. M. 1928, *Publ. Washburn Obs.*, **15**, 101.
Huffer, C. M., and Collins, G. W. 1962, *Astrophys. J., Suppl. Ser.*, **7**, 351.
Hut, P. 1981, *Astron. Astrophys.*, **99**, 126.
Jayasinghe, T., *et al.* 2019, *Mon. Not. Roy. Astron. Soc.*, **485**, 961 (https://www.asas-sn.osu.edu).
Johansen, K. T. 1971, *Astron. Astrophys.*, **12**, 165.
Jones, D. H. P. 1969, *Acta Astron.*, **19**, 53.
Jørgensen, H. E., and Grønbech, B. 1978, *Astron. Astrophys.*, **66**, 377.
Jørgensen, H. E., and Gyldenkerne, K. 1975, *Astron. Astrophys.*, **44**, 343.
Kallrath, J., and Milone, E. F. 2009, *Eclipsing Binary Stars: Modeling and Analysis*, 2nd ed., Springer, New York.
Khaliullin, Kh. F., and Kozyreva, V. S. 1989, *Astrophys. Space Sci.*, **155**, 53.
Kloppenborg, B. 2023, observations from the AAVSO International Database (https://www.aavso.org/databases).
Kopal, Z. 1959, *Close Binary Systems*, Chapman & Hall, London.
Kron, G. E. 1939, *Lick Obs. Bull.*, **19**, 59.
Kron, G. E. 1942, *Astrophys. J.*, **96**, 173.
Kron, G. E., and Gordon, K. C. 1953, *Astrophys. J.*, **118**, 55.
Krylov, A. V., Mossakovskaya, L. V., Khaliullin, Kh. F., and Khaliullina, A. I. 2003, *Astron. Rep.*, **47**, 551.
Lacy, C. H. 1981, *Astrophys. J.*, **251**, 591.
Lacy, C. H. S. 1993, *Astron. J.*, **105**, 1096.
Lacy, C. H. S. 1997, *Astron. J.*, **113**, 1091.
Lause, F. 1938, *Astron. Nachr.*, **266**, 237.
Lee, J.-W., Hong, K., and Kristiansen, M. H. 2020, *Publ. Astron. Soc. Japan*, **72**, 37.
Mallama, A. D. 1981, *Publ. Astron. Soc. Pacific*, **93**, 774.
Martin, W. C. 1938, *Bull. Astron. Inst. Netherlands*, **8**, 286.
Mayer, P., *et al.* 2016, *Astron. Astrophys.*, **591A**, 129.
McNamara, D. H. 1951, Ph.d. dissertation, Univ. California, Berkeley, CA.
Mossakovskaya, L. V. 1992, *Astron. Astrophys. Trans.*, **3**, 163.
NASA. 2023, NASA Exoplanet Archive (https://exoplanetarchive.ipac.caltech.edu).
Nordstrom, B., and Johansen, K. T. 1994, *Astron. Astrophys.*, **291**, 777.

O'Connell, D. J. K. 1935, *Publ. Riverview Coll. Obs.*, **1**, 11.
O'Connell, D. J. K. 1939, *Publ. Riverview Coll. Obs.*, **2**, 5.
O'Connell, D. J. K. 1948, *Mon. Not. Roy. Astron. Soc.*, **108**, 334.
O'Connell, D. J. K. 1967, *Ric. Astron.*, **7**, 339.
Pavlovski, K., Southworth, J., Kolbas, V., and Smalley, B. 2014, *Mon. Not. Roy. Astron. Soc.*, **438**, 590.
Perryman, M. A. C., *et al.* 1997, *Astron. Astrophys.*, **323**, L49 (https://www.cosmos.esa.int/web/hipparcos/catalogues).
Plavec, M. 1960, *Bull. Astron. Inst. Czechoslovakia*, **11**, 197.
Pojmański, G., Pilecki, B., and Szczygiel, D. 2005, *Acta Astron.*, **55**, 275 (http://www.astrouw.edu.pl).
Popper, D. M. 1988, *Astron. J.*, **95**, 190.
Popper, D. M., and Carlos, R. 1970, *Publ. Astron. Soc. Pacific*, **82**, 762.
Provoost, P. 1980, *Astron. Astrophys., Suppl. Ser.*, **40** 129.
Sabby, J. A., Sandberg Lacy, C. H., Ibanoglu, C., and Claret, A. 2011, *Astron. J.*, **141**, 195.
Schmitt, J. H. M. M. 1998, *Astron. Astrophys.*, **333**, 199.
Schmitt, J. H. M. M., *et al.* 2016, *Astron. Astrophys.*, **586A**, 104.
Semeniuk, I. 1968, *Acta Astron.*, **18**, 1.
Shakura, N. I. 1985, *Soviet Astron. Lett.*, **11**, 224.
Shappee, B. J., *et al.* 2014, *Astrophys. J.*, **788**, 48.
Southworth, J., Bruntt, H., and Buzasi, D. L. 2007, *Astron. Astrophys.*, **467**, 1215.
Southworth, J., Maxted, P. F. L., and Smalley, B. 2004, *Mon. Not. Roy. Astron. Soc.*, **351**, 1277.
Stebbins, J. 1911, *Astrophys. J.*, **34**, 112.
Stebbins, J. 1921, *Astrophys. J.*, **54**, 81.
Stebbins, J. 1928, *Publ. Washburn Obs.*, **15**, 41.
TESS Asteroseismic Science Operations Center (TASC). 2023, TESS Data for Asteroseismology (https://tasoc.dk/).
Tomkin, J., and Popper, D. M. 1986, *Astron. J.*, **91**, 1428.
Tremko, J., Papousek, J., and Vetesnik, M. 1978, *Astron. Inst. Slovak Acad. Sci.*, **159**, 199.
Tucker, R. S., Sowell, J. R., Williamon, R. M., and Coughlin, J. L. 2009, *Astron. J.*, **137**, 2949.
van Hamme, W. 1993, *Astron. J.*, **106**, 2096.
van Houten, C. J., van Houten-Groeneveld, I., van Genderen, A. M., and Kwee, K. 2009, *J. Astron. Data*, **15**, 2.
Volkov, I. M. 2020, *Contrib. Astron. Obs. Skalate Pleso*, **50**, 635.
Volkov, I. M. 2005, *Astrophys. Space Sci.*, **296**, 105.
Wilson, R. E., and Devinney, E. J., 1971, *Astrophys. J.*, **166**, 605.
Williamon, R. M. 1975, *Astron. J.*, **80**, 976.
Williams, J. G. 1994, *Astron. J.*, **108**, 711.
Woodward, E. J., and Koch, R. H. 1987, *Astrophys. Space Sci.*, **129**, 187.